

Research Article

Control of Chaotic Calcium Oscillations in Biological Cells

Quanbao Ji¹ and Min Ye² 

¹School of Mathematics and Physics, Guangxi University for Nationalities, Nanning 530006, Guangxi, China

²School of Education Science, Guangxi University for Nationalities, Nanning 530006, Guangxi, China

Correspondence should be addressed to Min Ye; 44225749@qq.com

Received 29 September 2020; Revised 29 October 2020; Accepted 21 January 2021; Published 4 February 2021

Academic Editor: Zhouchao Wei

Copyright © 2021 Quanbao Ji and Min Ye. This is an open access article distributed under the Creative Commons Attribution License, which permits unrestricted use, distribution, and reproduction in any medium, provided the original work is properly cited.

The contribution of this present paper is to propose a method that combines a chemical Brusselator reaction-diffusion system with a biological cell system via gap junction for controlling and visualizing the frequency and magnitude of chaotic intracellular calcium oscillations in two cell types, including nonexcitable cells and the glial cells. This produces a wide variety of oscillatory behaviors similar to those reported in numerous biological experiments. We particularly show that in the majority of chaos cases, the reactor to cell coupling can induce the generation of regular calcium oscillations as the coupling strength is varied. Together with the proposed method of coupled models, the regularity of these chaotic oscillations enables us to gain better understanding and extensive insights into the overall coupling dynamics.

1. Introduction

Cell is characterized by basic structural and functional unit, as seen under the electron microscope in tissues of organisms. As the most important chemical signals in the cytosol of living cells, calcium ion (Ca^{2+}) is indispensable for biological signaling pathway in various physiological activities of human body and participates in many physiological functions, such as heart beat discrimination, muscle contraction, and gene expression [1–4]. Different types of Ca^{2+} oscillations, which are encoded into complex and diverse biological signals through the variation of calcium flux, induce brain plasticity in two ways simultaneously, amplitude modulation and frequency modulation [5–10].

In contrast with nonexcitable cell, glia, which are approximately 10 times more in number than nonexcitable cell, are unable to generate similar response by an electrical signal. It is well-known that glia has no electrically excitable effects on the plasma membrane [11]. Trying to explain the dynamical mechanism of chaotic Ca^{2+} oscillation in nonexcitable cell and glia, a lot of mathematical models were established in the field of calcium signaling with purpose of investigating various types of Ca^{2+} oscillations in the experiment (for review, see [12]). In recent years, many chaos

control methods, such as adaptive control, feedback control, fuzzy control, and sliding mode control are proposed.

Here, we focus on a new approach that can help to control intracellular chaotic Ca^{2+} oscillation amplitude and frequency from a mathematical point of view in two types of cell systems. On this neurophysiological basis of their finds, mathematical models of control associated with membrane ion channels were discussed for describing different types of Ca^{2+} oscillations [13–23]. The question remains whether the dynamical mechanism correlated by system parameter is efficient for controlling the intracellular oscillations in glia. Therefore, it is becoming increasingly clear that assent to creation of precise chaotic Ca^{2+} regulation is interesting, since the process can reveal the dynamical mechanism of regular and chaotic attractors controlled by the system parameter.

2. Mathematical Models

The aim of the present paper is to investigate reversible control of the amplitude and the frequency of chaotic Ca^{2+} oscillation in two different kinds of mathematical models proposed by Borghans et al., Lavrentovich and Hemkin, and Zhao et al. as examples that regulate the intracellular chaotic

calcium oscillations [24–26]. The evolution of Borghans model is governed by the following equations:

$$\begin{cases} \frac{dX}{dt} = J_{in} + J_{leak} - J_{pump} + J_{er} - J_{out}, \\ \frac{dY}{dt} = J_{pump} - J_{leak} - J_{er}, \\ \frac{dZ}{dt} = J_A - J_D - J_C, \end{cases} \quad (1)$$

where

$$\begin{aligned} J_{in} &= k_{in1}r + k_{in2}, \\ J_{leak} &= rk_{leak} \frac{Z^4}{Z^4 + K_a^4} \times \frac{Y^2}{Y^2 + K_y^2} \times \frac{X^4}{X^4 + K_z^4}, \\ J_C &= eZ, \\ J_{er} &= k_f Y, \\ J_{pump} &= k_{kump} \frac{X^2}{X^2 + K_2^2}, \\ J_{out} &= k_{out} X, \\ J_A &= rk_p, \\ J_D &= k_d \frac{X^4}{X^4 + K_d^4} \times \frac{Y^2}{Y^2 + K_p^2}. \end{aligned} \quad (2)$$

There are three variables that represent the dynamics of nonexcitable cell model proposed by Borghans et al.: the free Ca^{2+} concentrations in the cytosol (X), the free Ca^{2+} concentrations in ER (Y), and inositol trisphosphate (IP_3) concentration in the cytosol (Z). Between cytosol and ER, most of Ca^{2+} fluxes were considered: leak Ca^{2+} from ER into cytosol (J_{leak}), Ca^{2+} uptake from cytosol into ER (J_{pump}), and Ca^{2+} from ER into cytosol (J_{er}). The parameter r denotes the stimuli level from outer space through the membrane of nonexcitable cell and into the cytosol, and hence we choose this parameter to be the control parameter to regulate the calcium oscillatory behaviors. Most of other parameter values used here are taken from our previous literatures in Ref. [18, 21, 22].

A mathematical one-pool model proposed by Lavrentovich et al. is also considered as another example of manipulating chaotic Ca^{2+} oscillation in glia cell type. Three differential equations in the Lavrentovich model form the relationship between the same variables appearing in the Borghans model.

$$\begin{cases} \frac{dCa_{cyt}}{dt} = v_{in} - k_{out} Ca_{cyt} + v_{CICR} - v_{serca} + k_f (Ca_{er} - Ca_{cyt}), \\ \frac{dCa_{er}}{dt} = v_{serca} - v_{CICR} - k_f (Ca_{er} - Ca_{cyt}), \\ \frac{dIP_3}{dt} = v_{PLC} - k_{deg} IP_3, \end{cases} \quad (3)$$

where

$$\begin{aligned} v_{serca} &= v_{M2} \left(\frac{Ca_{cyt}^2}{Ca_{cyt}^2 + k_2^2} \right), \\ v_{PLC} &= v_p \left(\frac{Ca_{cyt}^2}{Ca_{cyt}^2 + k_p^2} \right), \\ v_{CICR} &= 4v_{M3} \left(\frac{k_{CaA}^n Ca_{cyt}^n}{(Ca_{cyt}^n + k_{CaA}^n)(Ca_{cyt}^n + k_{CaI}^n)} \right) \\ &\quad \times \left(\frac{IP_3^m}{IP_3^m + k_{ip3}^m} \right) \times (Ca_{er} - Ca_{cyt}). \end{aligned} \quad (4)$$

This model considers the IP_3 receptor influenced by cytosolic Ca^{2+} which at low Ca^{2+} concentration activates the probability of receptor opening. The parameter v_{in} denotes the Ca^{2+} flow from outside into the glia membrane. By changing value of this parameter, we can mimic spontaneous Ca^{2+} oscillations appearing in biological experiments [23]. We investigated stability dynamics of the Lavrentovich model using similar values of most parameters in our previous studies for derivation [21, 22].

The current paper is aimed at proposing a method to control chaotic Ca^{2+} oscillation by integrating cell model with the reactor via coupling. The Brusselator system is described by the following equations:

$$\begin{cases} \frac{dx}{dt} = -(b+1)x + ax^2y, \\ \frac{dy}{dt} = bx - ax^2y. \end{cases} \quad (5)$$

This integration seemly occurs via diffusion of Ca^{2+} in cytosolic and ER alternatively, as is illustrated in Figure 1 from our previous study.

Most often biological information is encoded in regulation, variations in magnitude or frequency, and spatial organization of intracellular Ca^{2+} . In this case, Ca^{2+} and IP_3 concentrations act as the co-stimuli to trigger Ca^{2+} releasing from IP_3 receptor, and we add the coupling term ($Xk_{c1} - xk_{c2}$) to the first equation in (1). In summary, this coupled nonexcitable cell model can be described as follows:

$$\begin{cases} \frac{dX}{dt} = J_{in} + J_{leak} - J_{pump} + J_{er} - J_{out} - k_{C1}X + k_{C2}x, \\ \frac{dY}{dt} = J_{pump} - J_{leak} - J_{er}, \\ \frac{dZ}{dt} = J_A - J_D - J_C, \\ \frac{dx}{dt} = 1 - (b+1)x + ax^2y + k_{C1}X - k_{C2}x, \\ \frac{dy}{dt} = bx - ax^2y. \end{cases} \quad (6)$$

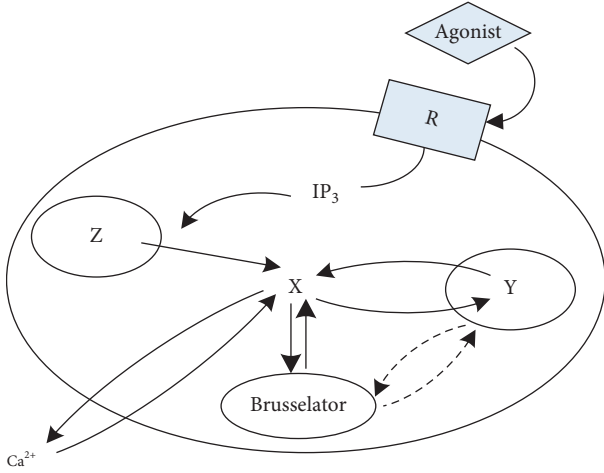


FIGURE 1: Schematic presentation of integration between the cell model and the Brusselator reactor. This illustration is from [19].

Having presented the artificial mathematical non-excitable cell model for controlling chaotic Ca^{2+} oscillation, we similarly couple the Brusselator reactor with glia cell system. This integrated coupling system is expressed as follows:

$$\left\{ \begin{array}{l} \frac{d\text{Ca}_{\text{cyt}}}{dt} = v_{\text{in}} - k_{\text{out}}\text{Ca}_{\text{cyt}} + v_{\text{CICR}} - v_{\text{serca}} + k_f(\text{Ca}_{\text{er}} - \text{Ca}_{\text{cyt}}) \\ -k_{\text{C1}}\text{Ca}_{\text{cyt}} + k_{\text{C2}}x, \\ \frac{d\text{Ca}_{\text{er}}}{dt} = v_{\text{serca}} - v_{\text{CICR}} - k_f(\text{Ca}_{\text{er}} - \text{Ca}_{\text{cyt}}), \\ \frac{d\text{IP}_3}{dt} = v_{\text{PLC}} - k_{\text{deg}}\text{IP}_3, \\ \frac{dx}{dt} = 1 - (b+1)x + ax^2y + k_{\text{C1}}\text{Ca}_{\text{cyt}} - k_{\text{C2}}x, \\ \frac{dy}{dt} = bx - ax^2y. \end{array} \right. \quad (7)$$

In our modified models, chaotic Ca^{2+} oscillation can be easily controlled by changing the parameter values of k_{C1} and k_{C2} , representing the assumed Ca^{2+} flux transport rate both in cytosol and Brusselator reactor, due to the involved variables and coupling of elements.

3. Results

In this section, we investigate possible method for controlling chaotic Ca^{2+} oscillation for understanding the dynamical mechanism. Furthermore, it is not only to control the magnitude and the frequency of chaotic Ca^{2+} oscillation in nonexcitable cell and glia but also to monitor the shape of chaos.

Firstly, we use equation (6) of the nonexcitable cell system to evaluate effectiveness of our method. Chaotic Ca^{2+} oscillations in the coupled system with the parameter $r=0.95$ are plotted in Figure 2. It is shown that chaotic Ca^{2+} oscillation occurs in this case. As the controlling rate parameters $k_{\text{C1}}=0$, $k_{\text{C2}}=0$, it means that the chemical Brusselator reactor has no effect on the coupled system (6). In Figure 2(a), it shows spiking chaos through complex dynamical activities. The 2D corresponding dimensional phase portrait diagram in (x, y, z) -plane is also plotted in Figure 2(b). One can easily see a basic attractor in the phase portrait.

Secondly, we fix the control parameters k_{C1} and k_{C2} to regulate the chaotic Ca^{2+} oscillations in nonexcitable cell system (6). In Figure 3(a), another spiking chaos can be gained by varying $k_{\text{C1}}=0.002$, $k_{\text{C2}}=0.04$, which is similar to that of Figure 2(a). The main difference is the way how the reduced small-amplitude level can be achieved, which is verified by the corresponding 2D phase diagram in Figure 3(b).

Based on the component-coupled method, an effective manipulation of chaotic Ca^{2+} oscillation is shown in Figure 4 when we choose $k_{\text{C1}}=0.1$ and $k_{\text{C2}}=0.1$. Compared with Figures 2(a) and 3(a), it can be seen that this kind of regulation significantly reduces the amplitude (see Figure 4(a)) and the calcium wave (see Figure 4(b)) in this case. There is a sharp decrease of spiking activity and distinctive shape variation of each chaotic spiking, which is followed by a slower decrease for high control parameter values. Therefore, we use the coupling method as a measure for manipulating the chaotic Ca^{2+} activities of the modified model.

We further examine the control properties of coupled system (6) for different values of controlling parameters k_{C1} and k_{C2} which determine the rate of amplitude and frequency of calcium flux. Figure 5(a) shows the corresponding time series of X for $k_{\text{C1}}=6$ and $k_{\text{C2}}=0.2$, respectively. When the value of k_{C1} and k_{C2} is large enough, the chaotic behavior turns to be a series of regular spiking. The main difference between them is that the phase portrait of spiking oscillation is a stable circle unlike the basic attractor in Figure 5(b). The transition is much different from that of previous time course in Figures 2(a), 3(a), and 4(a).

Finally, we use equation (7) of the glia cell system to test the validity of the coupling method. Time process of chaotic Ca^{2+} oscillations with the parameter $v_{\text{in}}=0.05025$ is shown in Figure 6(a). As $k_{\text{C1}}=0$, $k_{\text{C2}}=0$, it means similar to that in the coupled nonexcitable cell system (6).

The 3D dimensional phase portrait diagram in $(\text{Ca}_{\text{cyt}}, \text{Ca}_{\text{er}}, \text{IP}_3)$ -plane is also plotted in Figure 6(b), and one can easily see a strange attractor in the middle of portrait diagram.

In contrast with the original chaotic behavior, the shape of chaos in Figure 7(a) is of quite different spiking type as $k_{\text{C1}}=0.0001$, $k_{\text{C2}}=0.0001$, keeping their waveforms changed. The main difference is that this type of firing in Figure 7(a) is called the spiking chaos, while bursting chaos is considered in Figure 6(a). Burst means the system behavior alternates between repetitive firing and steady state, which is caused by the system slow variable. 3D dimensional phase portrait

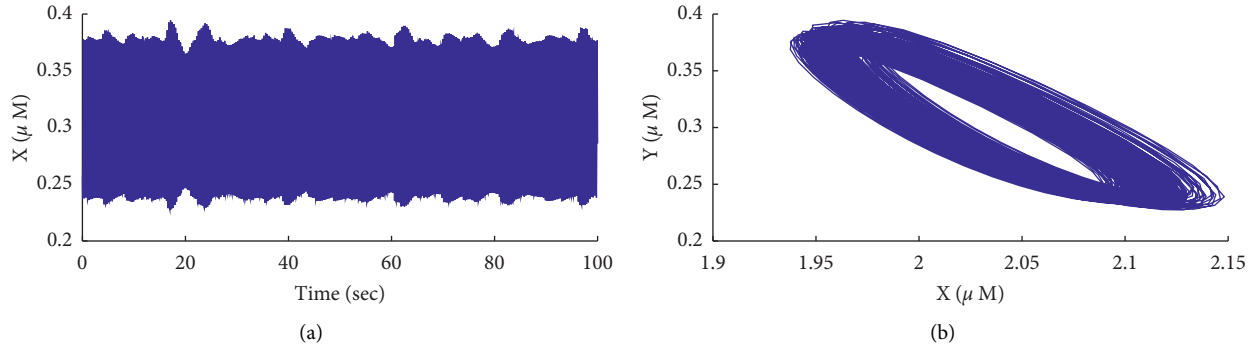


FIGURE 2: Original chaotic Ca^{2+} oscillation in coupled model (6) of nonexcitable cell without control constraints at $r=0.95$. (a) The respective time course of variable X with controlling rate parameters $k_{c1}=0$, $k_{c2}=0$. (b) 2D projection of the trajectory in X, Y phase space with controlling rate parameters $k_{c1}=0$, $k_{c2}=0$.

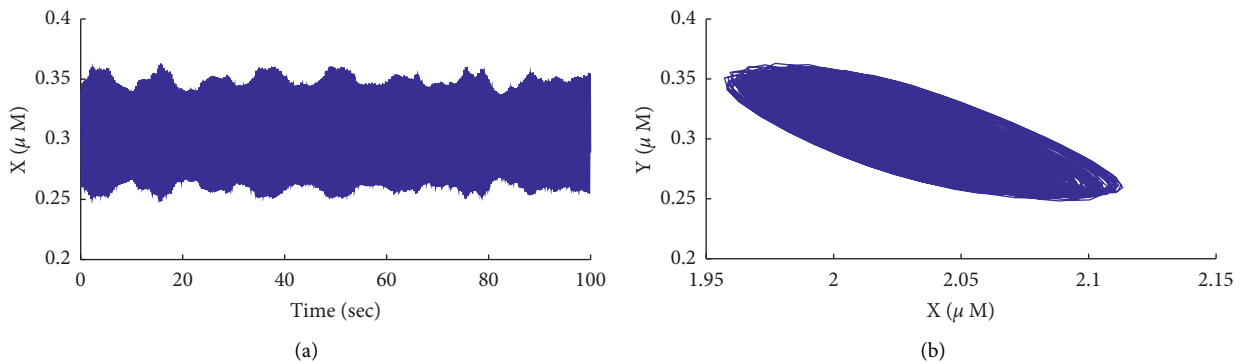


FIGURE 3: Small-amplitude feedback control of chaotic Ca^{2+} oscillation in coupled model (6) of nonexcitable cell at $r=0.95$. (a) The respective time course of variable X with controlling rate parameters $k_{c1}=0.002$, $k_{c2}=0.04$. (b) 2D projection of the trajectory in X, Y phase space with controlling rate parameters $k_{c1}=0.002$, $k_{c2}=0.04$.

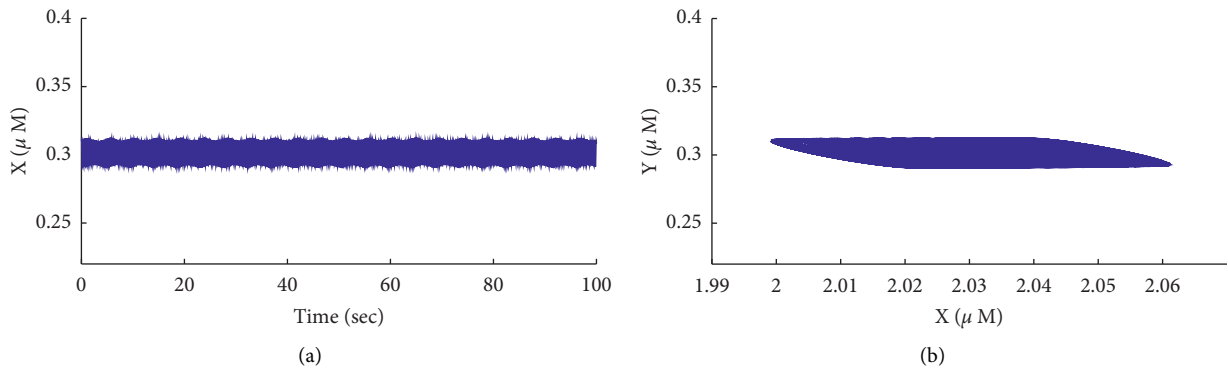


FIGURE 4: Large-amplitude feedback control of chaotic Ca^{2+} oscillation in coupled model (6) of nonexcitable cell at $r=0.95$. (a) The respective time course of variable X with controlling rate parameters $k_{c1}=0.1$, $k_{c2}=0.1$. (b) 2D projection of the trajectory in X, Y phase space with controlling rate parameters $k_{c1}=0.1$, $k_{c2}=0.1$.

diagram is drawn in Figure 7(b). More additional portrait circles occur.

When the parameters $k_{c1}=0.001$, $k_{c2}=0.01$, the coupled glia cell model begins to burst with quiet different chaotic behavior from the above one with time process shown in Figures 6(a) and 7(a). The results of numerical integration

for controlling chaotic calcium flux are shown in Figure 8. Figure 8(a) shows a typical example of burst in a sharp peak, which is followed by several lower frequency oscillatory activities. Figure 8(b) shows the three-dimensional portrait diagram corresponding to Figure 8(a). This type of oscillation is also a regular bursting.

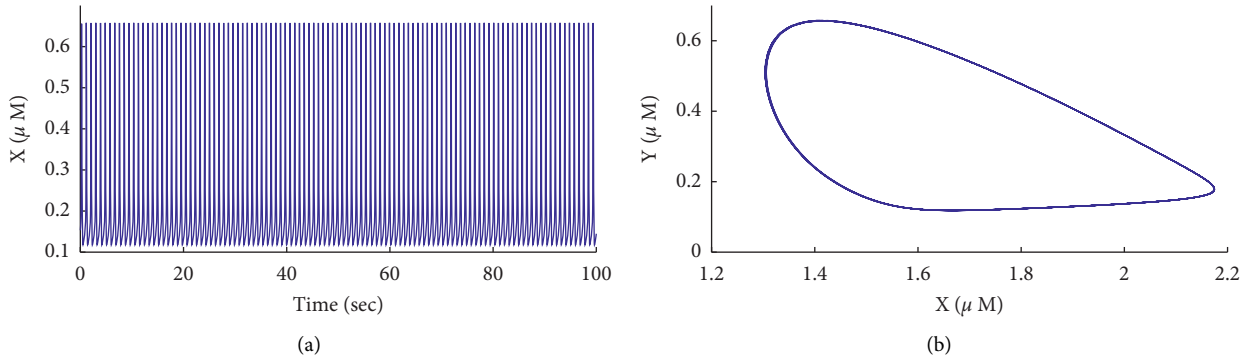


FIGURE 5: Shape, amplitude, and frequency control of chaotic Ca^{2+} oscillation in coupled model (6) of nonexcitable cell at $r = 0.95$. (a) The respective time course of variable X with controlling rate parameters $k_{c1} = 6$, $k_{c2} = 0.2$. (b) 2D projection of the trajectory in X, Y phase space with controlling rate parameters $k_{c1} = 6$, $k_{c2} = 0.2$.

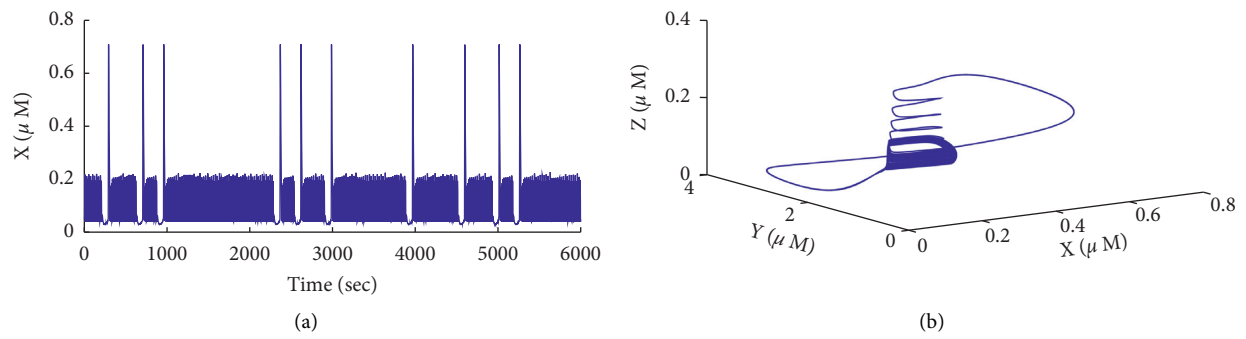


FIGURE 6: Original chaotic Ca^{2+} oscillation in coupled model (7) of the glia cell system without control constraints for the parameter $v_{in} = 0.05025$. (a) The respective time course of variable Ca_{cyt} with controlling rate parameters $k_{c1} = 0$, $k_{c2} = 0$. (b) 3D projection of the trajectory in $(\text{Ca}_{cyt}, \text{Ca}_{cyt}, \text{IP}_3)$ phase space with controlling rate parameters $k_{c1} = 0$, $k_{c2} = 0$.

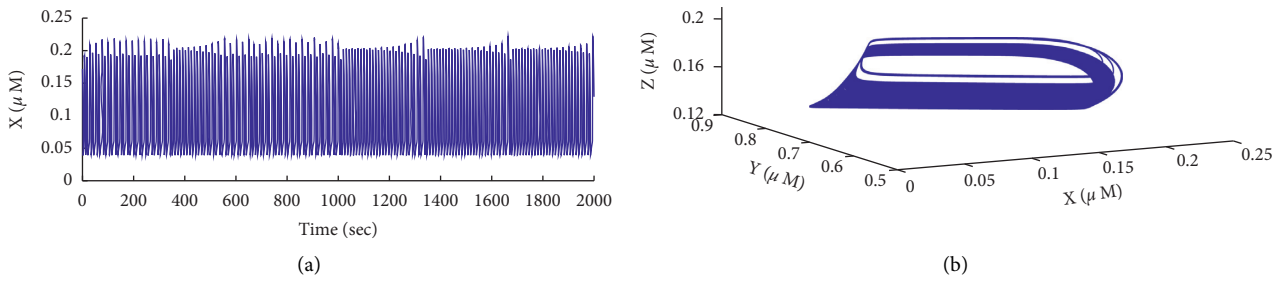


FIGURE 7: Shape and amplitude control of chaotic Ca^{2+} oscillation in coupled model (7) of the glia cell system for the parameter $r_{in} = 0.05025$. (a) The respective time course of variable Ca_{cyt} with controlling rate parameters $k_{c1} = 0.0001$, $k_{c2} = 0.0001$. (b) 3D projection of the trajectory in $(\text{Ca}_{cyt}, \text{Ca}_{cyt}, \text{IP}_3)$ phase space with controlling rate parameters $k_{c1} = 0.0001$, $k_{c2} = 0.0001$.

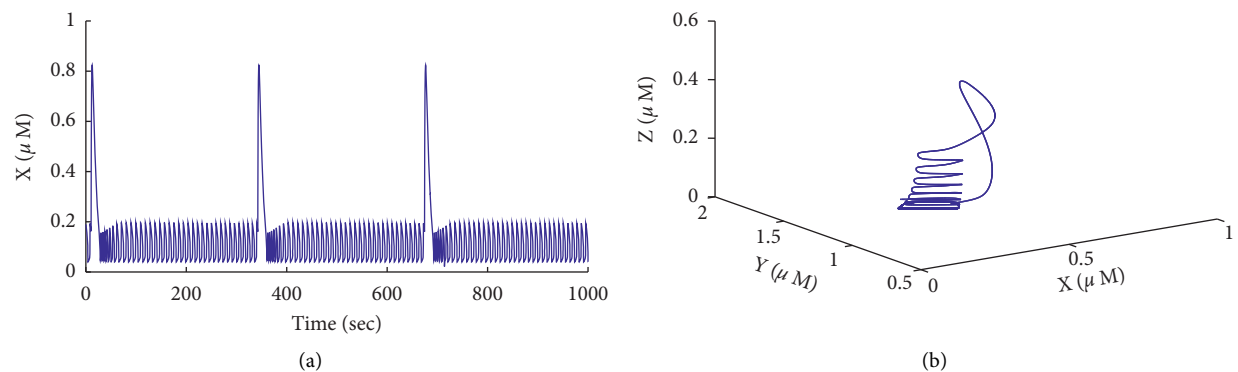


FIGURE 8: Shape, amplitude, and magnitude control of chaotic Ca^{2+} oscillation in coupled model (7) of the glia cell system for the parameter $r_{in} = 0.05025$. (a) The respective time course of variable Ca_{cyt} with controlling rate parameters $k_{c1} = 0.001$, $k_{c2} = 0.01$. (b) 3D projection of the trajectory in $(\text{Ca}_{cyt}, \text{Ca}_{cyt}, \text{IP}_3)$ phase space with controlling rate parameters $k_{c1} = 0.001$, $k_{c2} = 0.01$.

4. Summary

In summary, we have theoretically integrated a chemical Brusselator reactor to the nonexcitable cell and glia models, respectively, based on the coupling method. We aimed at controlling the chaotic Ca^{2+} oscillations. A component-coupled method was introduced by integrating a Brusselator reactor to cell model. This kind of integration not only influences the frequency and magnitude of chaotic calcium flux but also changes the shape of chaotic behavior. The integration method should be regarded as the initial effort for regulating intracellular chaotic Ca^{2+} oscillations in living cells. Validity of this coupling method was verified by changing values of controlling rate, respectively.

Therefore, simulation results in this paper may enhance our understanding of generation and transition mechanism of chaotic Ca^{2+} oscillations in nonexcitable cell and glia cell, which help us better understand the essence of calcium signaling between nonexcitable cell and the glia cell from a mathematical point of view.

Data Availability

The data used to support the findings of this study are included within this article, and the sources from where they were adopted were cited accordingly.

Conflicts of Interest

The authors declare that they have no conflicts of interest.

Authors' Contributions

The authors claim that the research was realized in collaboration with the same responsibility. All authors read and approved the last version of the manuscript.

Acknowledgments

This study was supported by the National Natural Science Foundation of China under grant nos. 12062004 and 11872084 and the Guangxi Natural Science Foundation under grant no. 2020JJA110010.

References

- [1] M. V. Sofroniew and H. V. Vinters, "Astrocytes: biology and pathology," *Acta Neuropathologica*, vol. 119, no. 1, pp. 7–35, 2010.
- [2] T. R. Chay, "Electrical bursting and luminal calcium oscillation in excitable cell models," *Biological Cybernetics*, vol. 75, no. 5, pp. 419–431, 1996.
- [3] J. Sneyd, K. Tsaneva-Atanasova, D. I. Yule, J. L. Thompson, and T. J. Shuttleworth, "Control of calcium oscillations by membrane fluxes," *Proceedings of the National Academy of Sciences*, vol. 101, no. 5, pp. 1392–1396, 2004.
- [4] J. F. Aguilar, K. L. Abro, K. Olusola, and Y. Ahmet, "Chaos in a calcium oscillation model via Atangana-Baleanu operator with strong memory," *The European Physical Journal Plus*, vol. 134, p. 140, 2019.
- [5] P. Hannanta-anan and B. Y. Chow, "Optogenetic control of calcium oscillation waveform defines NFAT as an integrator of calcium load," *Cell Systems*, vol. 2, no. 4, pp. 283–288, 2016.
- [6] M. Marhl, T. Haberichter, M. Brumen, and R. Heinrich, "Complex calcium oscillations and the role of mitochondria and cytosolic proteins," *Biosystems*, vol. 57, no. 2, pp. 75–86, 2000.
- [7] T. Haberichter, M. Marhl, and R. Heinrich, "Birhythmicity, trirhythmicity and chaos in bursting calcium oscillations," *Biophysical Chemistry*, vol. 90, no. 1, pp. 17–30, 2001.
- [8] E. Smedler and P. Uhlén, "Frequency decoding of calcium oscillations," *Biochimica et Biophysica Acta (BBA)-General Subjects*, vol. 1840, no. 3, pp. 964–969, 2014.
- [9] V. V. Matrosov and V. B. Kazantsev, "Bifurcation mechanisms of regular and chaotic network signaling in brain astrocytes," *Chaos: An Interdisciplinary Journal of Nonlinear Science*, vol. 21, no. 2, Article ID 23103, 2011.
- [10] M. Marhl, S. Schuster, and M. Brumen, "Mitochondria as an important factor in the maintenance of constant amplitudes of cytosolic calcium oscillations," *Biophysical Chemistry*, vol. 71, no. 2-3, pp. 125–132, 1998.
- [11] M. Pekny and M. Nilsson, "Astrocyte activation and reactive gliosis," *Glia*, vol. 50, no. 4, pp. 427–434, 2005.
- [12] F. Oschmann, H. Berry, K. Obermayer, and K. Lenk, "From in silico astrocyte cell models to neuron-astrocyte network models: a review," *Brain Research Bulletin*, vol. 136, pp. 76–84, 2018.
- [13] T. J. Shuttleworth and O. Mignen, "Calcium entry and the control of calcium oscillations," *Biochemical Society Transactions*, vol. 31, no. 5, pp. 916–919, 2003.
- [14] F. Codazzi, M. N. Teruel, and T. Meyer, "Control of astrocyte Ca^{2+} oscillations and waves by oscillating translocation and activation of protein kinase C," *Current Biology*, vol. 11, no. 14, pp. 1089–1097, 2001.
- [15] A. Cornell-Bell, S. Finkbeiner, M. Cooper, and S. Smith, "Glutamate induces calcium waves in cultured astrocytes: long-range glial signaling," *Science*, vol. 247, no. 4941, pp. 470–473, 1990.
- [16] D. A. Zacharias, G. S. Baird, and R. Y. Tsien, "Recent advances in technology for measuring and manipulating cell signals," *Current Opinion in Neurobiology*, vol. 10, no. 3, pp. 416–421, 2000.
- [17] A. Pietak and M. Levin, "Bioelectrical control of positional information in development and regeneration: a review of conceptual and computational advances," *Progress in Biophysics and Molecular Biology*, vol. 137, pp. 52–68, 2018.
- [18] Y. Lu and Q. Ji, "Control of intracellular calcium bursting oscillations using method of self-organization," *Nonlinear Dynamics*, vol. 67, no. 4, pp. 2477–2482, 2012.
- [19] Q. Ji, Y. Zhou, Z. Yang, and X. Meng, "Evaluation of bifurcation phenomena in a modified Shen-arter model for intracellular Ca^{2+} and Ca^{2+} bursting oscillations," *Nonlinear Dynamics*, vol. 84, no. 3, pp. 1281–1288, 2016.
- [20] Q. Ji and Y. Lu, "Bifurcations and continuous transitions in a nonlinear model of intracellular calcium oscillations," *International Journal of Bifurcation and Chaos*, vol. 23, no. 2, Article ID 1350033, 2013.
- [21] M. Ye and H. K. Zuo, "Stability Analysis of regular and chaotic Ca^{2+} oscillations in astrocytes," *Discrete Dynamics in Nature and Society*, vol. 2020, Article ID 9279315, 9 pages, 2020.
- [22] H. Zuo and M. Ye, "Bifurcation and numerical simulations of Ca^{2+} oscillatory behavior in astrocytes," *Frontiers in Physics*, vol. 8, 2020.

- [23] I. Goto, S. Kinoshita, and K. Natsume, "The model of glutamate-induced intracellular Ca^{2+} oscillation and intercellular Ca^{2+} wave in brain astrocytes," *Neurocomputing*, vol. 58–60, pp. 461–467, 2004.
- [24] J. M. Borghans, G. Dupont, and A. Goldbeter, "Complex intracellular calcium oscillations A theoretical exploration of possible mechanisms," *Biophysical Chemistry*, vol. 66, no. 1, pp. 25–41, 1997.
- [25] M. Lavrentovich and S. Hemkin, "A mathematical model of spontaneous calcium(II) oscillations in astrocytes," *Journal of Theoretical Biology*, vol. 251, no. 4, pp. 553–560, 2008.
- [26] Y. Zhao, X. Sun, Y. Liu, and J. Kurths, "Phase synchronization dynamics of coupled neurons with coupling phase in the electromagnetic field," *Nonlinear Dynamics*, vol. 93, no. 3, pp. 1315–1324, 2018.